

A NOVEL SUB-MICRORADIAN BEAM DIAGNOSTIC AND ALIGNMENT SYSTEM

Carl G. Chen¹, Ralf K. Heilmann, Paul T. Konkola, G. S. Pati and Mark L. Schattenburg
*Space Nanotechnology Laboratory
Massachusetts Institute of Technology, Cambridge, MA 02139*

I. INTRODUCTION

By interfering a pair of millimeter-diameter laser beams, scanning beam interference lithography (SBIL) is capable of exposing linear gratings and grids in photoresist with extremely low phase distortions. (Please see our other paper [1] in these proceedings for a more detailed description of the SBIL architecture.) Our ultimate design goal calls for sub-nanometer accumulated phase distortions across a 300 mm substrate when compared to a grating with a perfect linear phase. These accurate periodic structures, when patterned onto ultra-low thermal expansion substrates, can be used as absolute metrology standards [2]. They may also enable advances in other fields such as the making of high precision optical encoders.

Elsewhere [3], we have demonstrated the ability to diagnose *in-situ* the spatial period and phase of a grating image via the use of interferometry. For a grating period of approximately 2 μm , we have reported a period measurement repeatability of three parts per ten thousand, one sigma, and a grating phase drift of 0.25 mrad/sec. Both the repeatability error and the phase drift are expected to decrease by three orders of magnitude after some major system upgrades, including the installation of an environmental enclosure and the addition of thermally stable metrology frames. Ultimately, the beam diagnostic system is capable of resolving the overall phase of a 1 mm radius grating to around 1 nm, corresponding to a period measurement accuracy of one part per million.

The diagnostic system is an integral part of a sub-microradian beam alignment system (Fig. 1 [4, 5]), which is composed of a series of beamsplitters, mirrors, lenses, position sensing detectors (PSD), and picomotors. The system is designed to sense beam position fluctuations and angle shifts with resolutions of 61 nm and 61 nrad, respectively. Based on the sensor readings, a network of eight picomotors, each with an angular resolution of 0.74 μrad , adjusts four tip-tilt steering mirrors so as to overlap the beams in position and to equalize their incident angles, thus setting the grating period and ensuring vertical fringes. To obtain good fringe contrast, beam centroids must be overlapped to within a small fraction of the beam radius, typically 1%, which corresponds to 10 μm for a 1 mm radius beam. A PSD located in the substrate plane is used to directly verify the beam overlap with a resolution of 61 nm. Slow drifts in the lithography station, thermal or otherwise, once diagnosed, can be corrected by periodically registering the beams to a reference beamsplitter cube on the interferometer stage [3], ensuring ultra-low phase distortions. The approach is similar to that used in electron-beam mask writers [6] whereby in order to compensate for drifts, the electron beam is periodically referenced to a fiducial mark on the stage.

II. SYSTEM DESIGN

Data acquisition from the PSDs is handled by two National Instruments 6034E 16-bit I/O boards. The PSD used to sense the beam overlapping in the plane of the substrate is an

¹Email: gangchen@mit.edu

On-Trak Photonics UV2L4 duolateral position sensing detector. To rid the errors that may be introduced if the beam reflects multiple times off the PSD's protective window, we have acquired a special no-window version of the detector. Once the beams are overlapped, the picomotors, purchased from New Focus, Inc., are driven so as to equalize the incident angles, without shifting the positions of the beams at the substrate.

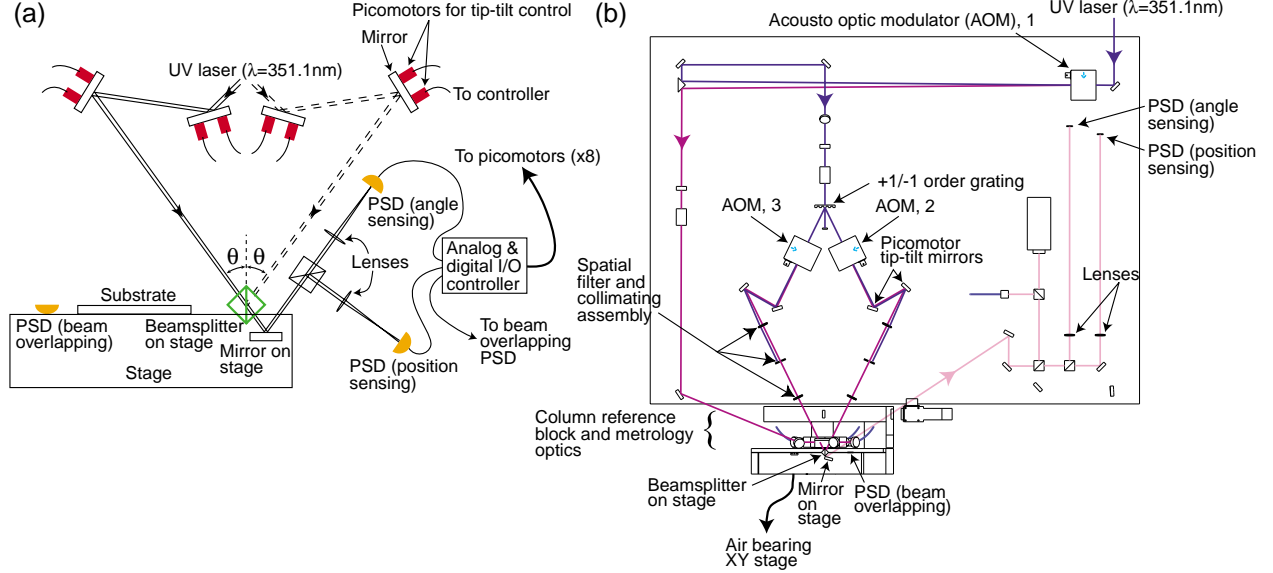


Figure 1: (a) A schematic of the SBIL beam alignment system. The PSD used for beam overlapping, the substrate, a reference beamsplitter cube and a steering mirror are attached to the interferometer stage. All other components are attached to an optical bench. During beam diagnostics and alignment, the stage is moved so that the beams intersect the cube as shown. (b) Actual design of the alignment system. The grating beamsplitter provides greater tolerance on the beam angular instability and temporal coherence than the traditional cube beamsplitter. Three acousto optic modulators (AOM) provide digital heterodyne interference fringe control. Furthermore, by nulling AOM 2 and 3 control signals, each beam can be individually shuttered to provide position and angle readouts.

The alignment system adopts the same position and angle decoupling topology as that described in our earlier work [4]. The theory of angle decoupling is straightforward. After passing through a thin lens of focal length f , a beam's angle (α), not its position, is converted to a displacement (r) at the back focal plane of the lens, where $r = f\alpha$. Position decoupling is best understood via the ABCD matrix formalism [7]. Defined in Fig. 2(a), the output position and angle of the beam, r and r' , can be written in terms of the input beam position and angle, d and α , geometric distances L_0 and L_1 , and the focal length f ,

$$\begin{aligned} \begin{pmatrix} r \\ r' \end{pmatrix} &= \begin{pmatrix} 1 & L_1 \\ 0 & 1 \end{pmatrix} \begin{pmatrix} 1 & 0 \\ -1/f & 1 \end{pmatrix} \begin{pmatrix} 1 & L_0 \\ 0 & 1 \end{pmatrix} \begin{pmatrix} d \\ \alpha \end{pmatrix} \\ &= \begin{pmatrix} 1 & L_1 \\ 0 & 1 \end{pmatrix} \begin{pmatrix} 1 & 0 \\ -1/f & 1 \end{pmatrix} \begin{pmatrix} 1 & L_0 - \Delta \\ 0 & 1 \end{pmatrix} \begin{pmatrix} d + \Delta\alpha \\ \alpha \end{pmatrix}. \end{aligned} \quad (1)$$

Therefore, if L_0 and L_1 are chosen such that the beam's position at the output plane (r) is only a function of the position at the input plane (d), then this particular choice of position decoupling is strictly maintained across all possible input planes. Two On-Trak Photonics UV2L2 duolateral PSDs are used as position and angle sensors, with resolutions of 61 nm and 61 nrad, respectively, limited by the resolution of the 16-bit I/O board.

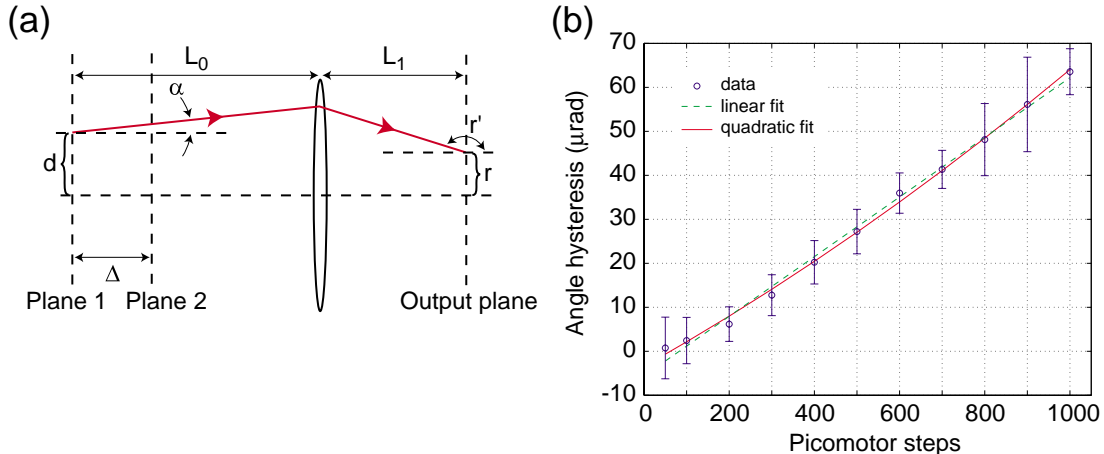


Figure 2: (a) Position decoupling. (b) Picomotor repeatability study. For each data point, the picomotor is first commanded forward by the indicated number of steps, then backward by the same number of steps. Difference between the initial and final angles is recorded by the angle sensing PSD. Before a new set of measurement, the picomotor is commanded so as to return the beam spot to the same location on the PSD. This is to ensure that the starting load on the picomotor remains the same for all measurements.

The picomotors have a displacement resolution of better than 30 nm, which translates into an angular adjustability of $0.74 \mu\text{rad}$. The technology enables us to equalize the incident beam angles and correct for beam drifts with sub-microradian accuracy, which is necessary given a one-part-per-million overall phase distortion budget [4]. Each beam is steered in position and angle by four picomotors, interfaced to a New Focus Picomotor Driver (Model 8732), which is itself controlled via external TTL signals from a National Instruments PCI-DIO-96 digital I/O board. Analog and digital control algorithms have been implemented using LabVIEW. Prior to the actual alignment, each of the four picomotors is commanded in sequence to move by an amount. The recorded position and angle data is used to compute a calibration matrix. Once the system is calibrated, we can then coordinate picomotor movements in order to equalize the angles while maintaining the beam overlap.

Due to the nature of its frictional drive, a picomotor's step size varies. As shown in Fig. 2(b), motions in opposite directions by the same number of steps are not equivalent. Repeatability is thus an issue with the picomotors. Open-loop control of the alignment system is impractical. One can not, for example, calibrate the system using a fixed number of picomotor steps as a calibration unit, since the device behaves unrepeatably. We implement a close-loop controller which calibrates not to a unit of picomotor step, but to a unit of sensor distance. The latter is an invariant, assuming we can effectively control drifts of thermal, vibrational, mechanical and acoustic origins. Prior to the alignment, each of the four picomotors is stepped until the beam intensity has decreased by 10% on the position sensor, in other words, the beam has started to fall off the sensor. (Because of the particular optical topology that we are using, the beam always falls off the position sensor first.) The position and angle readouts before and after the picomotor movement help define a 'unit' vector, which is expressed in terms of sensor distances. In this fashion, a 4×4 calibration matrix can be obtained, without any link to picomotor step size. During alignment, an individual picomotor is commanded to move till a desired sensor output is obtained. This effectively rids the picomotor non-repeatability pitfall. For speed, a successive approximation type of algorithm is implemented to drive the picomotors, much similar to that used on most

A/D converters [8]. Special care is taken such that the beams never fall off the two sensors while any one of the picomotors is driven.

III. CONCLUSIONS AND FUTURE WORK

We have constructed a system to satisfy the need of microradian level beam angle alignment during scanning beam interference lithography. Analog and digital control algorithms have been implemented based on a close-loop control scheme that effectively circumvents the problem of picomotor step non-repeatability. Critical testing of the system will be carried out once major upgrades to SBIL, such as the installation of an environmental enclosure and thermally stable metrology frames, are done. Latest test results will be presented.

IV. ACKNOWLEDGMENTS

We gratefully acknowledge the outstanding student, staff, and facility supports from the Space Nanotechnology Laboratory. This work was supported by DARPA under Grant No. DAAG55-98-1-0130 and NASA under Grant No. NAG5-5271.

REFERENCES

1. P. T. Konkola, C. G. Chen, R. K. Heilmann, G. S. Pati, and M. L. Schattenburg, "Scanning Beam Interference Lithography," these proceedings.
2. M. L. Schattenburg, C. Chen, P. N. Everett, J. Ferrera, P. Konkola, and H. I. Smith, "Sub-100 nm metrology using interferometrically produced fiducials," *J. Vac. Sci. Technol. B* **17**, 2692–2697 (1999).
3. C. G. Chen, P. T. Konkola, R. K. Heilmann, G. S. Pati, and M. L. Schattenburg, "Image metrology and system controls for scanning beam interference lithography," to be published in *J. Vac. Sci. Technol. B*, Nov/Dec 2001.
4. P. T. Konkola, C. G. Chen, R. K. Heilmann, and M. L. Schattenburg, "Beam steering system and spatial filtering applied to interference lithography," *J. Vac. Sci. Technol. B* **18**, 3282–3286 (2000).
5. R. K. Heilmann, P. T. Konkola, C. G. Chen, G. S. Pati, and M. L. Schattenburg, "Digital heterodyne interference fringe control system," to be published in *J. Vac. Sci. Technol. B*, Nov/Dec 2001.
6. H. Pearce-Percy, R. Prior, F. Abboud, A. Benveniste, L. Gasiosek, M. Lubin, and F. Raymond, "Dynamic corrections in MEBES 4500," *J. Vac. Sci. Technol. B* **12**, 3393–3398 (1994).
7. H. A. Haus, in *Waves and fields in optoelectronics* (Prentice-Hall, Inc., 1984), Chap. 5.
8. P. Horowitz and W. Hill, in *The art of electronics*, 2nd ed. (Cambridge University Press, 1989), Chap. 9.